Supporting Information

Water Oxidation Catalysis by Co(II) Impurities in Co(III)$_4$O$_4$ Cubanes

Andrew M. Ullman,[†] Yi Liu,[†] Michael Huynh,[†] D. Kwabena Bediako,[†] Hongsen Wang,[‡] Bryce L. Anderson,[†] David C. Powers,[†] John J. Breen,[§] Héctor D. Abruña,[‡] and Daniel G. Nocera[†]

[†]*Department of Chemistry and Chemical Biology, Harvard University, 12 Oxford Street, Cambridge, MA 02138*

[‡]*Baker Laboratory, Department of Chemistry and Chemical Biology, Cornell University, Ithaca, NY 14853*

[§]*Department of Chemistry and Biochemistry, Providence College, 1 Cunningham Square, Providence, RI 02918*

Email: dnocera@fas.harvard.edu

Table of Contents

Experimental Methods

Materials. $Co(NO_3)_2 \cdot 6H_2O$ (Alfa Aesar), sodium acetate (Sigma-Aldrich), pyridine (Sigma-Aldrich), methyl isonicotinate (Sigma-Aldrich), ethylenediaminetetracarboxylic acid tetrasodium salt dehydrate (Sigma-Aldrich), $Ru(bpy)_3Cl_2 \cdot 6H_2O$ (Sigma-Aldrich), sodium persulfate (Sigma-Aldrich), and ammonium cerium(IV) nitrate (Sigma-Aldrich) were purchased and used as received. Buffer solutions were made from KH_2PO_4 (Mallinckrodt) using 18 MΩ cm distilled water from a MilliPore purification system. Synthesis of crude $Co_4O_4(OAc)_4(py)_4$, crude **1**, was performed according to the procedures of Dismukes[1] and Bonchio & coworkers.[2] Synthesis of crude $Co_4O_4(OAc)_4(py\text{-}COOMe)_4$, crude **1-COOMe**, was performed according to the procedure of Das.[3]

Purification and Characterization of 1 and 1-COOMe. Purification of the compounds **1** and **1-COOMe** was performed on a Biotage Isolera One automated flash chromatography system using a mobile phase gradient of 2–10% methanol/dichloromethane. A typical loading ratio was 10 mg of crude material for 1 g of silica. Samples were loaded onto the columns using a minimal volume of dichloromethane. Typical yields after purification were 40–50%. Proton nuclear magnetic resonance (^1H NMR) spectra were acquired on an Agilent DD2-600 (600 MHz) instrument and chemical shifts are referenced to residual protium in the NMR solvent (HDO = δ 4.79). Mass spectroscopic (MS) data were acquired on a Bruker micrO-TOF-QII LCMS ESI-TOF mass spectrometer in the positive ion mode. All mass spectra were externally calibrated with sodium formate. Elemental analysis was performed by Midwest Microlabs (Indianapolis, IN).

Synthesis of Oxidized Cobalt Cubane, [1]PF$_6$. Purified **1** (75.5 mg, 0.0886 mmol) was dissolved in 10 mL of acetonitrile. In a separate vial, 1.1 eq of $(NH_4)_2Ce(IV)(NO_3)_6$ (53.4 mg, 0.0974 mmol) was dissolved in 3 mL of acetonitrile. To a the stirring solution of **1** was added the Ce(IV) solution in a dropwise manner. The mixture darkened and was stirred at room temperature for 30 min. The mixture was concentrated under reduced pressure and redissolved in 8 mL of DI water. To this aqueous solution was added a solution of 452 mg of KPF_6 in 5 mL of DI water, which resulted in a precipitation of the product. This precipitate was filtered over a 5 μm nylon filter paper, washed with 10 mL of ice water, and then 20 mL of diethyl ether. The solid was dried under reduced pressure resulting in a dark green solid (66.4 mg, 0.0666 mmol, 75.1 % yield). ^1H NMR of this sample in CD_3CN exhibited paramagnetically broadened peaks: 10.10 (12 H), 6.63 (8 H), 6.16 (4 H), 2.68 (very broad, 8 H). Crystals suitable for X-ray diffraction from a synchrotron source were grown by vapor diffusion of diethyl ether into an acetonitrile solution of **[1]PF$_6$**.

1   McCool, N. S.; Robinson, D. M.; Sheats, J. E.; Dismukes, G. C. *J. Am. Chem. Soc.* **2011**, *133*, 11446–11449.

2   Berardi, S.; La Ganga, G.; Natali, M.; Bazzan, I.; Puntoriero, F.; Sartorel, A.; Scandola, F.; Campagna, S.; Bonchio, M. *J. Am. Chem. Soc.* **2012**, *134*, 11104–11107.

3   Chakrabarty, R.; Bora, S. J.; Das, B. K. *Inorg. Chem.* **2007**, *46*, 9450–9462.

Single Crystal XRD. The structure of **1[PF$_6$]** (Figure S1) was collected on a Bruker three-circle platform goniometer equipped with an Apex II CCD and an Oxford cryostream cooling device at 15 K. Radiation was supplied from a synchrotron source (0.41328 Å). Crystal was mounted on a glass fibre using Paratone N oil. Data were collected as a series of φ scans. Data were integrated using SAINT[4] and scaled with a multi-scan absorption correction using SADABS. The structures were solved by intrinsic phasing methods using SHELXS-97 and refined against F^2 on all data by full matrix least squares with SHELXL-97.[5] All non-hydrogen atoms were refined anisotropically. Hydrogen atoms were placed at idealized positions and refined using a riding model.

Electrochemical Methods. All electrochemical experiments were recorded at ambient temperature with a CH Instrument 760D or 730C potentiostat. A BASi Ag/AgCl reference electrode was used in all cases. In the cyclic voltammogram (CV) experiments the counter electrode was a Pt wire, while in the bulk electrolysis experiments a Pt mesh was used. In the CV experiments, 3 mm diameter glassy carbon working electrodes were used predominately as well as in specific experiments 2 mm diameter platinum and gold electrodes. These were cleaned by polishing on felt with 1 µm alumina followed by 0.3 µm alumina, and then sonication in 18 MΩ cm distilled water, rinsing with acetone and drying with compressed air. For the bulk electrolysis experiments, glassy carbon plate electrodes were used (25 × 5 × 1 mm). These electrodes were cut from a 25 × 25 × 1 mm plate (SPI Supplies) using a diamond saw. The FTO electrodes were cleaned by sonication in acetone followed by rinsing in 18 MΩ cm distilled water.

Photochemical Oxidation Method. Photochemical experiments were performed using a 1000 W high-pressure Hg/Xe arc lamp (Oriel), with a beam passed through a water immersed 0.4 OD filter, a 400 nm long-pass filter, an iris, and a water-jacketed cuvette holder. The solution O_2 concentrations were measured using a fluorescence-based O_2 sensor (Ocean Optics) fitted with a FOXY probe. Calibration of the probe was performed using two points, ambient air, $[O_2]$ = 253 µM, and after bubbling N_2 for 15 min, $[O_2]$ = 0 µM. The probe was inserted through the cap of the cuvette using a perforated septa and needle. In the dark, a 2 mL photochemical sample was made from stock solutions of $[Ru(bpy)_3^{2+}]$ = 2 mM, $[S_2O_8^{2-}]$ = 70 mM, and [**1**] = 1.32 mM all in 0.1 M KP$_i$ buffer (pH = 7) using 0.5 mL, 1 mL, and 0.5 mL from the respective stocks, resulting in the final concentrations, $[Ru(bpy)_3^{2+}]$ = 0.5 mM, $[S_2O_8^{2-}]$ = 35 mM, and [**1**] = 0.33 mM. Nitrogen was bubbled through the sample for 15 min before being exposed to the beam. The samples were stirred vigorously throughout the irradiation period.

DEMS (Differential Electrochemical Mass Spectrometry). DEMS experiments were conducted on a home-designed/assembled DEMS system that has a detecting limit of ~0.1

---

4   Bruker AXS (2009). Apex II. Bruker AXS, Madison, Wisconsin.

5   Sheldrick, G. M. *Acta Cryst.* **2010**, *D66*, 479-485.

nmol. The DEMS system has been described in details in a previous publication.[6] Briefly, the DEMS setup consists of two differentially pumped chambers (ionization chamber and analysis chamber) and a quadruple mass spectrometer (QMS 220 M1, PrismaPlus, Pfeiffer Vacuum). The main and analysis chambers were pumped by a Pfeiffer 65 L/s and a Varian 250 L/s turbomolecular pumps, respectively, which were backed by a rotary vane pump (DUO 10 M, Pfeiffer Vacuum). The PrismaPlus™ quadruple mass spectrometer was connected to the analysis chamber and equipped with electron multiplier/faraday cup dual detecting units. The time constant of the mass spectrometer was in the millisecond regime.

A special dual thin layer flow electrochemical cell made of Kel-F was connected to the ionization chamber via an angle valve for the DEMS experiment. The construction of this cell can be found elsewhere.[7] There are two compartments: the upper one for electrochemical reaction and the lower one for mass spectrometric detection, which are connected through 6 capillaries. In the upper compartment, the working electrode was pressed against a ~100 mm thick Teflon gasket with an inner diameter of 6 mm. This leaves an exposed area of 0.28 cm^2 and results in an electrolyte volume of ~ 3 μL. In the lower compartment, a porous Teflon membrane (Gore-Tex) supported on a stainless steel frit served as the interface between the electrolyte and vacuum. It was pressed against a ~100 mm thick Teflon gasket with an inner diameter of 6 mm. The Gore-Tex Teflon membrane had a mean thickness of ~ 75 μm, a mean pore size of 0.02 μm and a porosity of 50%. Two Pt wires at the inlet and outlet of the dual thin-layer flow cell, connected through an external resistance (0.2~3 MΩ), were used as counter electrodes. A Ag/AgCl electrode in saturated KCl solution, connected to the outlet of the DEMS cell through a Teflon capillary, served as reference electrode. The electrolyte flow was driven by the hydrostatic pressure in a supply bottle (flow rate 7–10 μL/s), which ensured fast transport of the species formed at the electrode to the mass spectrometric compartment, where the volatile products were evaporated into the vacuum system of the DEMS (time constant, ~1–2 s) through the porous Teflon membrane.

Electrochemical measurements during DEMS experiment were carried out with EG&G PAR Model 173 Potentiostat/Galvanostat, with an EG&G PAR Model 175 universal programmer to generate potential steps and triangular waveforms for cyclic voltammetry (CV). Electrochemical and mass spectrometric data were simultaneously recorded with a National Instrument DAQ board, using home-written data acquisition software in LabView. Freshly polished glassy carbon (GC) electrode was served as working electrode for all DEMS experiments. Typical CV profile was recorded from a 1 mM sample concentration in 0.1 M KP$_i$ pH 7 solution between +0.40 V and +1.50 V. The potential was scanned at the

---

[6] Wang, H.; Abruña, H. *Electrocatalysis of Direct Alcohol Fuel Cells: Quantitative DEMS Studies, in Fuel Cells and Hydrogen Storage*; Bocarsly, A.; Mingos, D. M. P., Eds.; Springer: Berlin, **2011**; vol. 141, pp 33–83.

[7] Baltruschat, H. *J. Am. Soc. Mass Spec.* **2004**, *15*, 1693–1706.

scan rate of 10 mV/s in the positive direction and at least 3 cyclic scans were performed to get the stable cyclic voltammograms.

EPR Spectroscopy. EPR spectra were recorded on a Bruker ELEXIS E-580 spectrometer equipped with a Bruker ER4122 SHQE-W1 resonator and an Oxford Instruments ESR 900 cryostat. All experiments were collected using field modulation of 10 G at 100 kHz and 2 mW microwave power at a temperature of 70 K.

Co(II) Induced ^{31}P NMR Line Broadening Analysis. Phosphorous nuclear magnetic resonance (^{31}P NMR) spectra were acquired on Varian Mercury400 (400 MHz) spectrometer with chemical shifts referenced to a 85% H_3PO_4 standard. A calibration curve of [Co(II)] versus the line width of phosphate ^{31}P NMR signal was created as follows. To a 1 mL NMR sample of 0.5 mM purified **1** in 0.2 M KP_i (pH = 7), 10 μL aliquots of a 2.5 mM:2.5 mM aqueous Co(OAc)$_2$:pyridine solution were added. After each addition, a ^{31}P NMR spectrum was acquired using enough transients to ensure sufficient signal to noise (Figure 7). The line width of the resulting ^{31}P signal was measured using the "dres" command in the VNMRJ data acquisition program. The experiment was repeated twice more to obtain a standard deviation of the average, Figure 7b. The Co(II) concentration of the three batches of **1** were assessed by measuring the FWHM of 0.426 mg/mL solutions (0.5 mM, assuming 100 % purity) in 0.2 M KP_i (pH = 7). Three samples were made from each batch and the average and standard deviation were calculated. [Co(II)] was then calculated using the equation derived from the linear regression in Figure 7b. Error was propagated in the usual way.[8]

Electron Microscopy of Electrode Surfaces. Microscopy samples were prepared from a bulk electrolysis of a solution of 1 mM analyte in 0.2 M KP_i pH = 7 buffer using GC plate electrodes described in the Electrochemical Methods section. The electrodes were masked with scotch tape to expose two 10 x 5 mm areas. The electrolysis was performed for 300 s under rapid (400 rpm) stirring for all samples. After completion of electrolysis, the electrodes were gently rinsed in 18 MΩ distilled water, air dried, and then dried under vacuum. Field emission scanning electron microscopy (FESEM) was performed with a Zeiss Supra55VP. The FESEM was operated at a beam voltage of 5 kV at a working distance of 8.5 mm with a 30 μm aperture and the InLens detector. Elemental quantification was determined at a beam voltage of 13 kV with an energy dispersive X-ray spectrometer (EDS from EDAX Inc.) using EDAX ZAF correction factors.

X-ray Photoelectron Spectroscopy (XPS). The presence of cobalt oxide on glassy carbon electrode surfaces after anodization in solutions of crude and purified **1** as well as without added **1** was examined using a Thermo Scientific K-Alpha XPS system. Samples were

---

8   Harris, D. C. *Quantitative Chemical Analysis*; W. H. Freeman: New York, 2003; Ch. 3.

illuminated with a monochromated Al Kα X-ray source (1486.6 eV energy and 0.85 eV line width) of 400 μm spot size. A low-energy (0 to 14 eV) electron flood gun was employed to mitigate surface charging. High-resolution spectra of the Co $2p_{1/2}$ and $2p_{3/2}$ peaks were collected from 750.5 to 832.5 eV using an energy step of 0.1 eV, dwell time of 50 ms, average of 20 scans, and a pass energy of 50 eV. All samples were calibrated to the C 1s (284.8 eV) peak.

Digital Simulation. The simulated CV was constructed using the data fitting function in the DigiElch software (version 7).[9] The background subtracted experimental data was imported into the program along with the relevant experimental conditions, such as area of the electrode, 0.0706 cm² (3 mm diameter) and the scan rate 0.1 V/s. A charge transfer couple was inputted into the fitting program with a nonvariable reduction potential equal to 1.054 V using the Butler-Volmer model of electrode kinetics with a transfer coefficient of α = 0.5. The program was then allowed to vary standard rate constant, k_s, and the diffusion coefficient, D. A satisfactory fit for the reversible couple in the three experimental CVs shown in Figure S10 was found with the values k_s = 0.008 cm/s and $D = 4 \times 10^{-6}$ cm²/s.

Calculating the Moles of Cobalt Needed to Account for Current in CVs of Purified 1. At high buffer concentrations, the current density (I) at a given overpotential (η) is related to the exchange current density (I_0) by the following equation:

$$\log I = \log I_0 + \frac{F}{RTln10}\eta \tag{1}$$

The exchange current density, however, depends on the thickness of the film, d_f, as has been extensively discussed.[10] The film thickness, d_f, is related to the exchange current density (I_0) through the following equation and set of constants:

$$I_0 = I_0^{max}\tanh\frac{d_f}{d_f^{opt}} \tag{2}$$

where $I_0^{max} = 1.75 \times 10^{-10} A/cm^2$ and is the current density when $d_f \rightarrow \infty$, and $d_f^{opt} = 1440\ nm$, which is the optimal film thickness. From the data in Figure S10, we measure an average current density at 1.5 V of the last sweep at $1.1 \pm 0.4 \times 10^{-4}$ A/cm² (using the last sweep avoids error from background subtraction, which more significantly affects the first sweeps). From this value, we calculate $d_f = 8.2 \times 10^{-7}$ nm using Eqs. 1 and 2, above. The film thickness can be correlated to moles of cobalt deposited using data from

[9] Rudolf, M. *J. Electroanal. Chem.* **2003**, *543*, 23–39; DigiElch from Elchsoft under http://www.elchsoft.com.

[10] Bediako, D. K.; Costentin, C.; Jones, E. C.; Nocera, D. G.; Savéant, J.-M. *J. Am. Chem. Soc.* **2013**, *135*, 10492–10502.

the experimental section of ref 10 of the SI, which leads to the following linear equation (with y-intercept fixed at 0) that relates film thickness to mC/cm² of charge passed:

$$\frac{mC}{cm^2} \text{ of Co deposition} = 0.148 \times d_f(nm) \tag{3}$$

which leads to a charge density of 1.2×10^{-7} mC/cm². This value can be converted to moles of deposited cobalt atoms by considering the area of the electrode (0.0707 cm²) and that each coulomb of charge equates to one cobalt atom. Thus, 9×10^{-8} nmol of cobalt, deposited as Co-OEC, could lead to a current density of 0.11 mA/cm² at 1.5 V vs. Ag/AgCl.

To make a meaningful comparison between the above value for the amount of cobalt needed to account for the observed current density and the amount of cobalt added to the electrochemical cell in the form of **1**, we must consider the amount of cobalt in the form of **1** that experienced the potential of the electrode surface, and not the entirety of the [**1**] in the CV cell. We can use the simulation software to attain a reliable estimate for this value by considering the concentration profile at 1.5 V vs. Ag/AgCl for the reversible couple, Figure S25. By integrating under the concentration profile for the oxidized species, we find that 4.85 nmol/cm² of **1** are oxidized to **1**⁺ over the course of a scan to 1.5 V, leading to 0.34 nmol of **1** once the area of the electrode is considered. Since there are four cobalt atoms per molecule of **1**, this leads to a fraction of **1** that would need to fully decompose to Co-OEC as:

$$\frac{9 \times 10^{-8} \text{ nmol Co atom}}{0.34 \text{ nmol } \mathbf{1} \times 4 \dfrac{\text{nmol Co atom}}{\text{nmol } \mathbf{1}}} = 6.6 \times 10^{-8} = 66 \text{ ppb}$$

Possible Level of O₂ Produced Electrochemically by the Cubane Cluster within the Error of Measurements. The average current density found at 1.5 V vs. Ag/AgCl for CVs of purified **1** on glassy carbon electrodes was 0.11 mA/cm² (red traces, Figures S10b–d). First, we assume that the entirety of this current is used for the four electron oxidation of H₂O to O₂ by the molecules of **1** that experience the anodic potential at the electrode surface. Thus, we can convert this value to a TOF, using Faraday's constant and the value for [**1**] at the electrode surface, which, as discussed in the previous section, can be attained using the simulation software (Figure S25).

$$0.11 \times 10^{-3} \frac{C}{s \times cm^2} \times \frac{mol\ e^-}{96485.3\ C} \times \frac{1\ mol\ O_2}{4\ mol\ e^-} = \frac{0.28\ nmol\ O_2}{s}$$

$$TOF = \frac{\dfrac{0.28\ nmol\ O_2}{s \times cm^2}}{\dfrac{4.85\ nmol\ \mathbf{1}}{cm^2}} = 0.058\ nmol/s$$

Table S1. Elemental Analysis Results for **1**

Element	Calcd.	**1** Batch A	**1** Batch B	**1** Batch C	**1** Purified
C	39.46	39.23	39.56	39.18	38.80
H	3.78	4.19	4.04	4.10	3.96
N	6.57	6.47	6.45	6.48	6.48

Table S2. Crystal data and structure refinement for $[Co_4O_4(OAc)_4(py)_4]PF_6$, **1[PF_6]**

Empirical formula	$C_{30}H_{35}Co_4N_5O_{12}PF_6$
Formula weight	1038.32
T (K)	15
λ (Å)	0.41328
Crystal system	Orthorhombic
Space group	*Pbca*
a (Å)	19.2399(15)
b (Å)	16.7691(13)
c (Å)	24.620(2)
α (°)	90
β (°)	90
γ (°)	90
V (Å^3)	7943.3(11)
Z	15
Abs. coeff (mm^{-1})	0.92
θ range for data collection (°)	1.654 - 26.370
Index ranges	$-19 \le h \le 24$; $-20 \le k \le 17$; $-30 \le l \le 30$
Reflections collected	70744
Independent reflns (R_{int})	8092 (0.059)
Data/restraints/parameters	8092/236/528
GOF[a] on F^2	1.211
R1[b] (I > 2σ)	0.0336
R1 (all data)	0.0527
wR2 (all data)	0.1187
Largest diff. peak, hole	1.10, –1.48

[a] GOF = $(\Sigma w(F_o^2 - F_c^2)^2/(n - p))^{1/2}$ where n is the number of data and p is the number of parameters refined.
[b] $R1 = \Sigma||F_o - |F_c||/\Sigma|F_o|$. [c] $wR2 = (\Sigma (w(F_o^2 - F_c^2)^2)/\Sigma (w(F_o^2)^2))^{1/2}$.
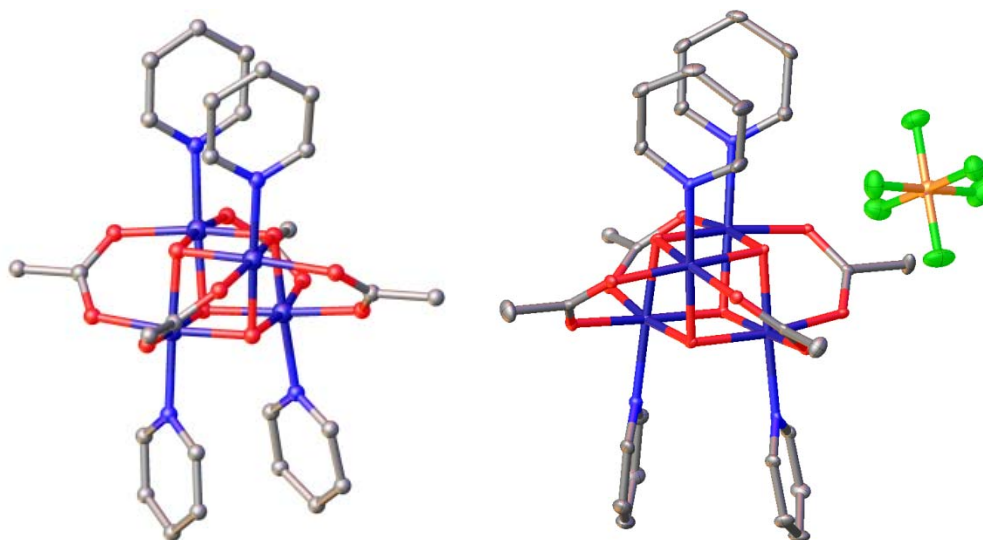
Figure S1. Thermal ellipsoid representation of (left) **1**, where the crystallographic data has been taken from ref 3 in the SI, and (right) **1[PF₆]** at the 50% probability level. Hydrogen atoms and an acetonitrile molecule have been omitted for clarity. Atoms are color-coded: gray (carbon), blue (nitrogen), red (oxygen), dark blue (cobalt), green (fluorine), and yellow (phosphorous).
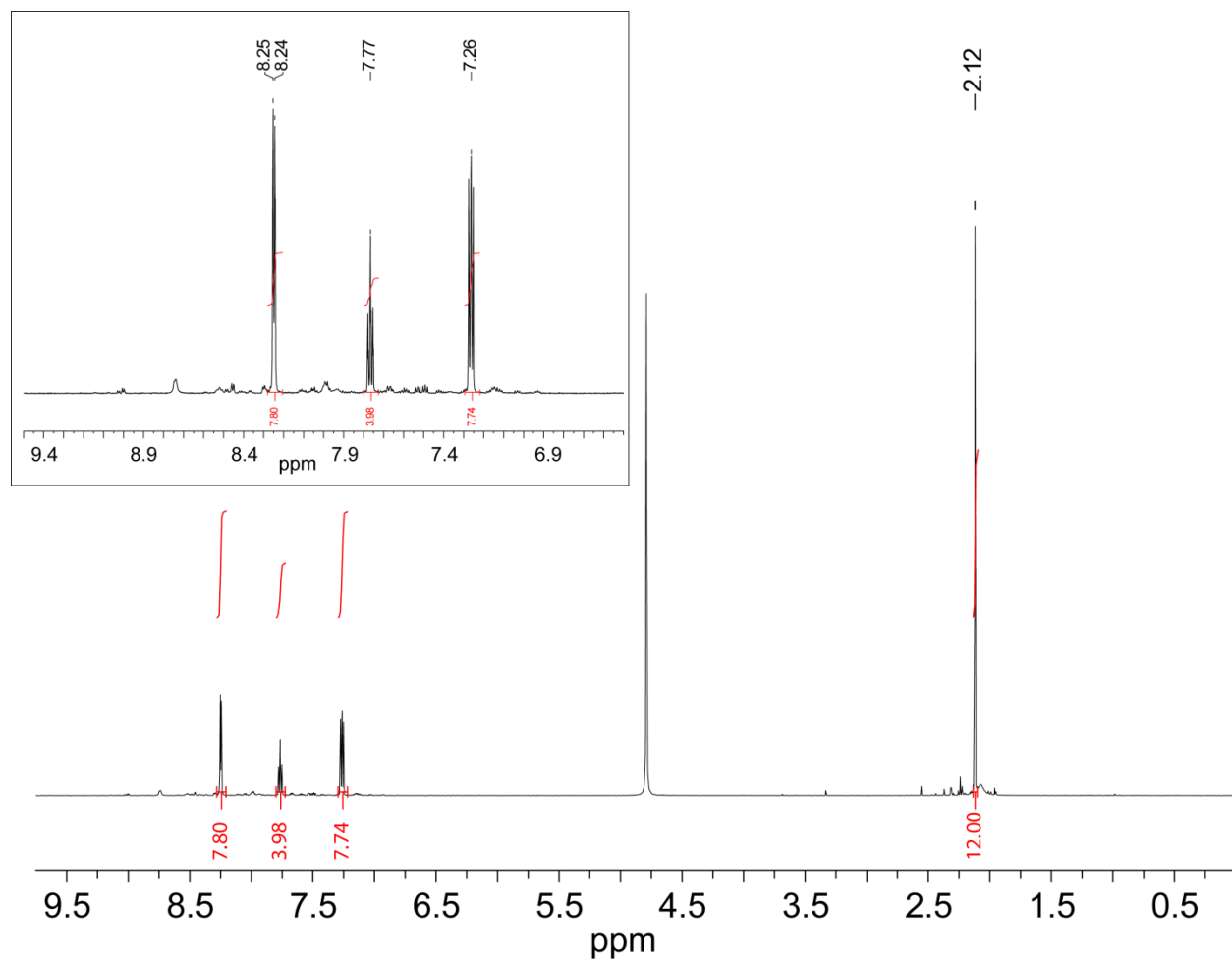
Figure S2. ^{1}H NMR spectrum of 10 mM crude **1** (Batch A) in D$_2$O. Inset: magnification of the aromatic region of the spectrum.
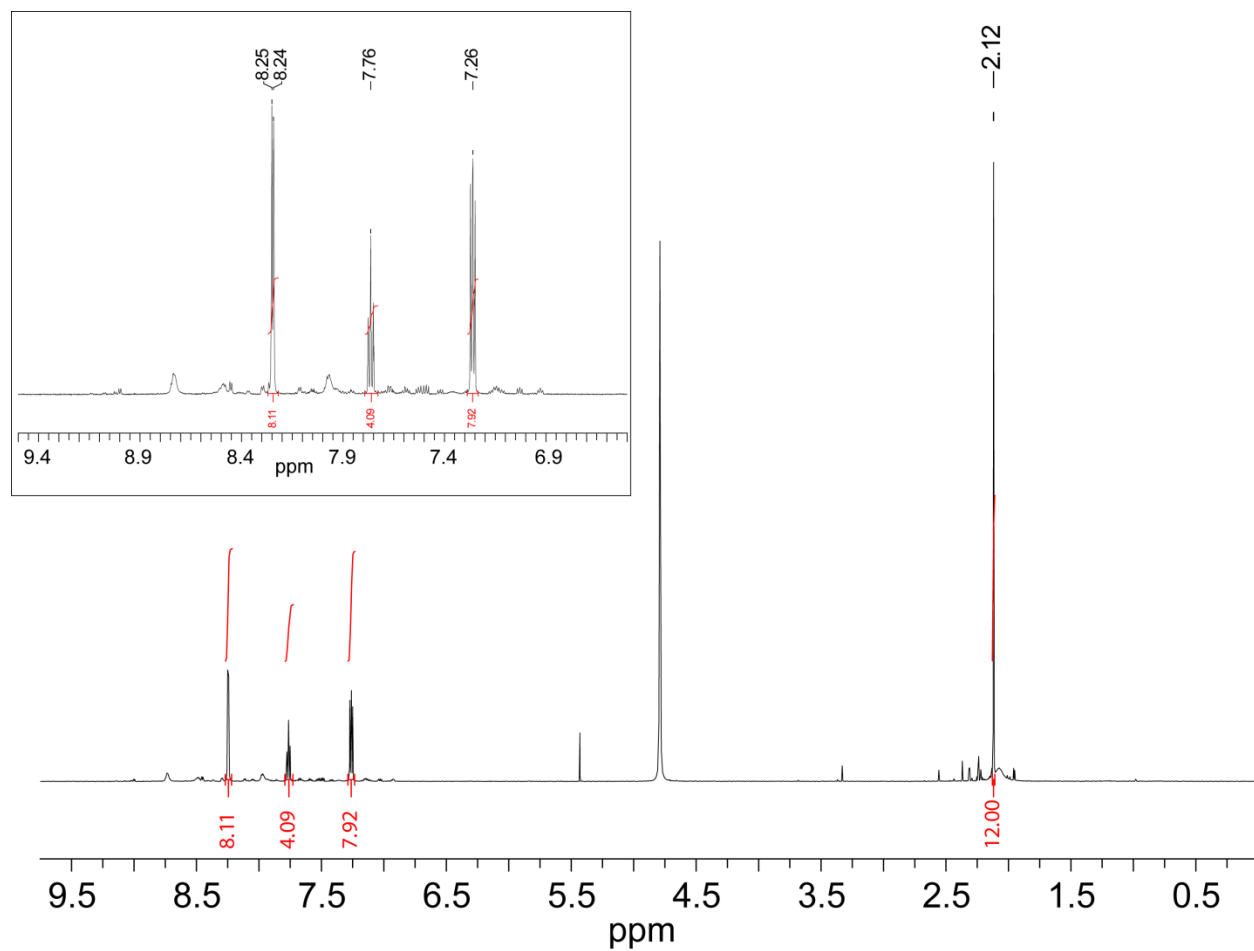
Figure S3. ^{1}H NMR spectrum of 10 mM crude **1** (Batch B) in D$_2$O. Inset: magnification of the aromatic region of the spectrum.
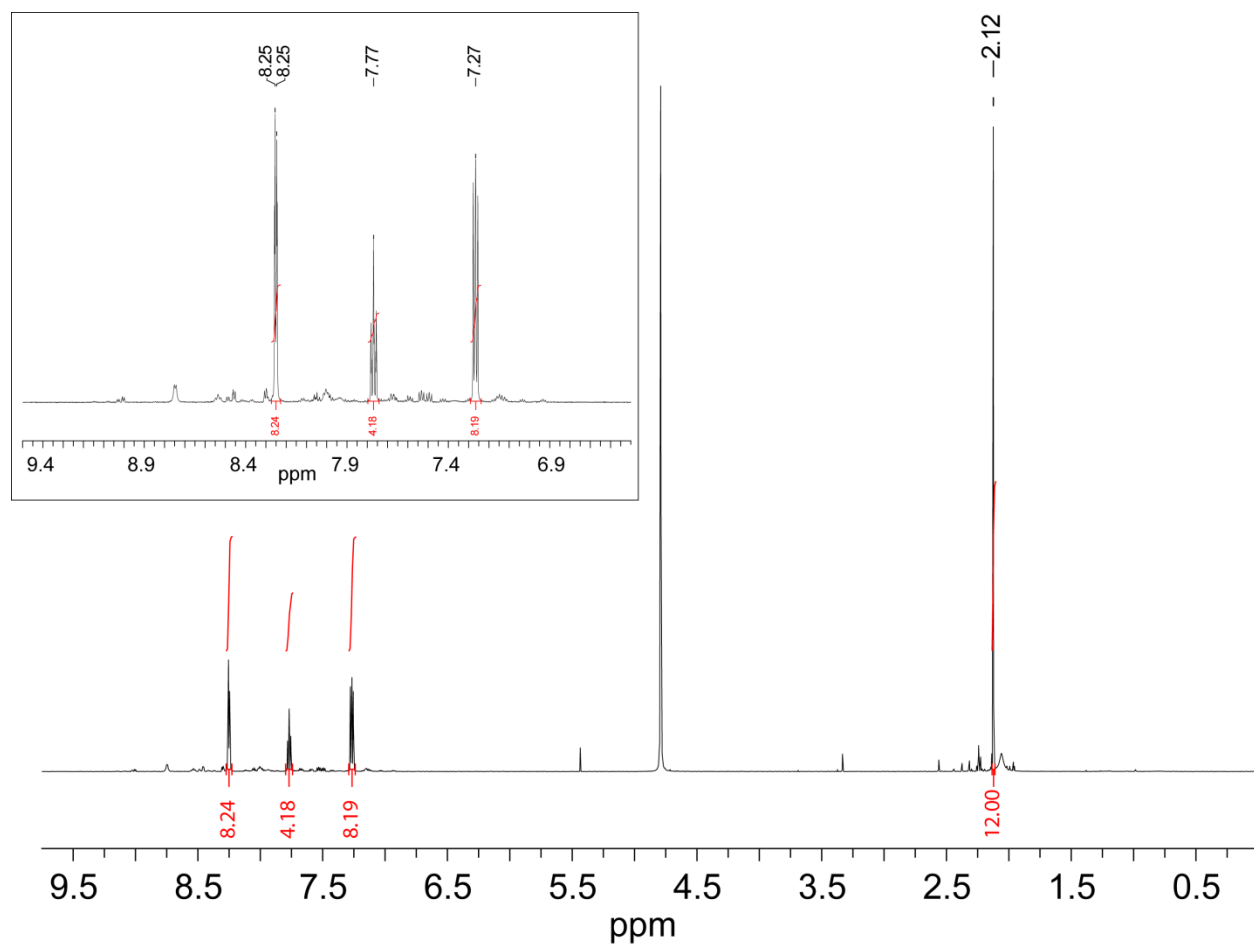
Figure S4. ^{1}H NMR spectrum of 10 mM crude **1** (Batch C) in D_2O. Inset: magnification of the aromatic region of the spectrum.
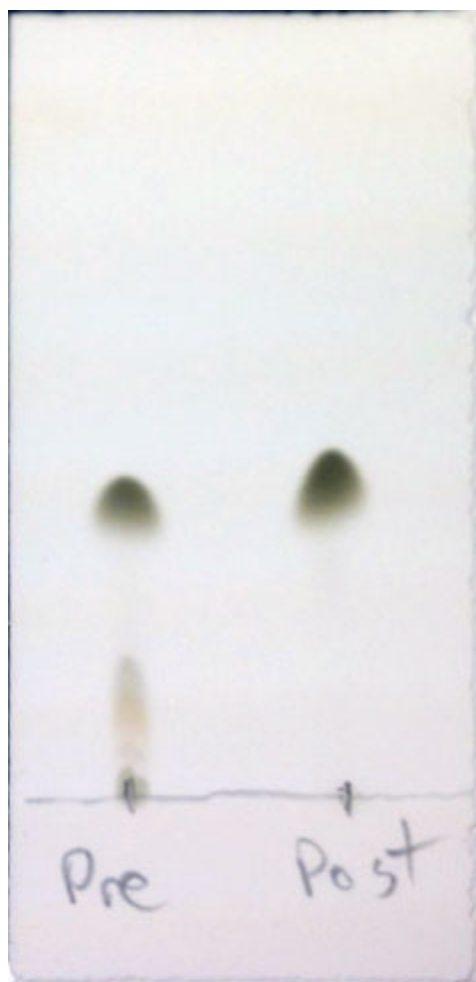
Figure S5. A comparison of TLC for left, crude **1**, and right, purified **1**, using a 5% methanol in dichloromethane mobile phase.
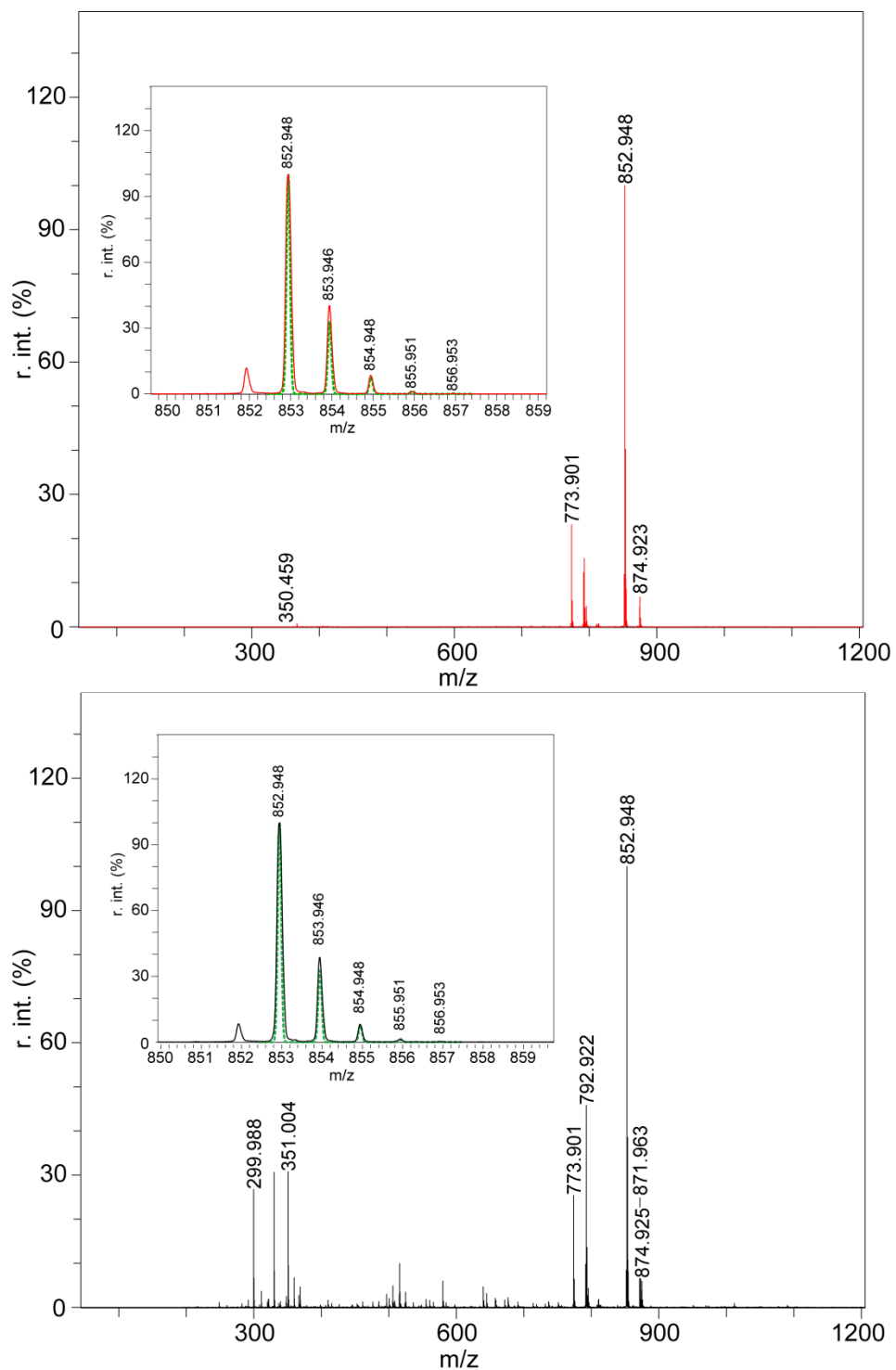
Figure S6. A comparison of the ESI mass spectra for top (red line, ▬) pure **1** and bottom (black line, ▬) crude **1**. The insets show a magnification of the most intense peak in each spectra at m/z = 852.948, which corresponds to **1** + H⁺. The dashed green line is the simulated spectrum for **1** + H⁺.
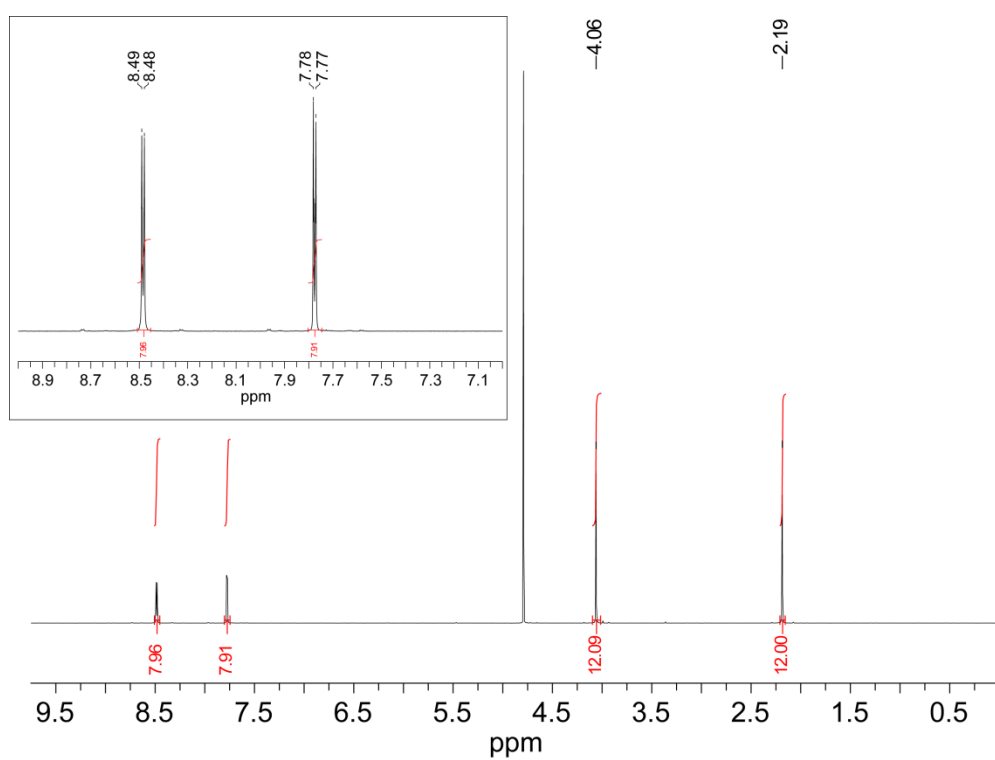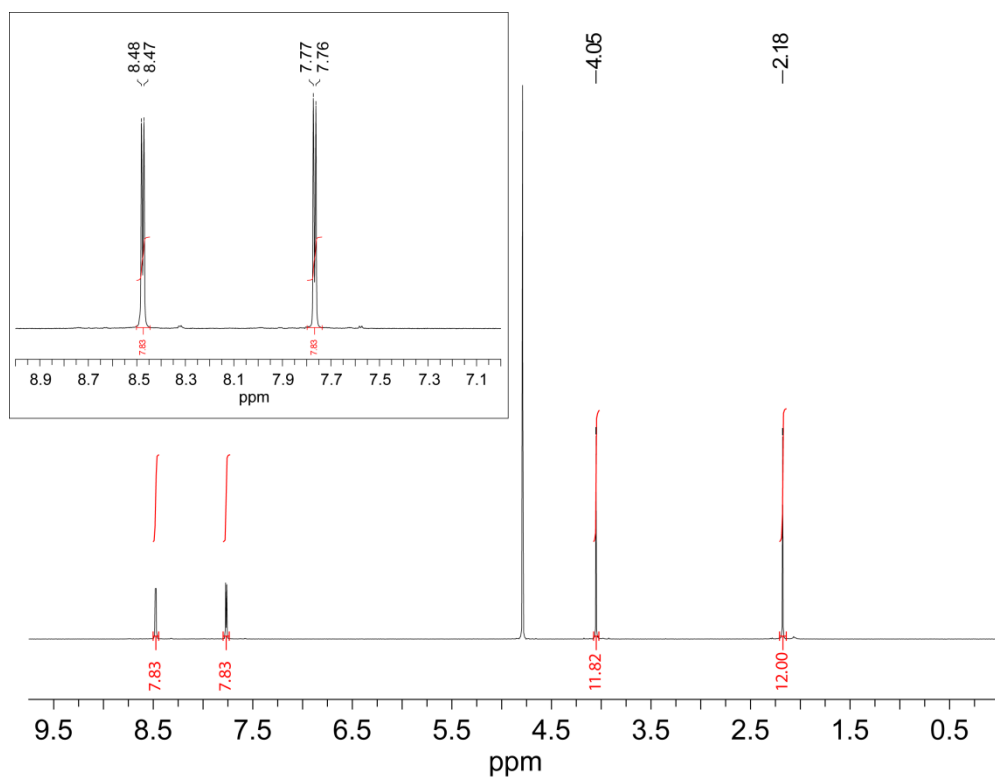
Figure S7. ^{1}H NMR spectrum of 10 mM (top) crude **1-COOMe** and (bottom) purified **1-COOMe** in D$_2$O. Inset: magnification of the aromatic region of the spectrum.
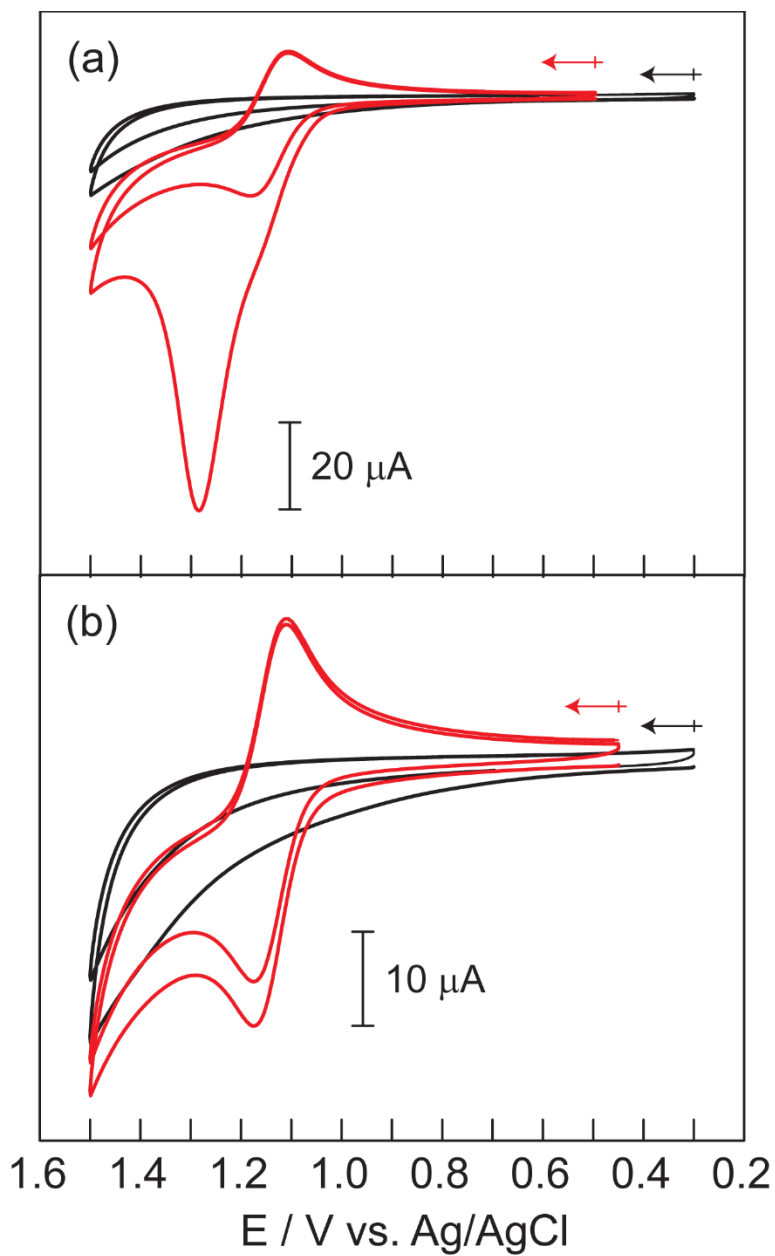
Figure S8. (a) CVs showing two full scans of (red line, ━) 2 mM crude **1-COOMe** and (black line, ━) no analyte in 0.2 M KP$_i$ (pH = 7). (b) CVs showing two full scans of (red line, ━) 2 mM pure **1-COOMe** and (black line, ━) no analyte in 0.2 M KP$_i$ (pH = 7). The arrows and crosses indicate the initial point and direction of scans.
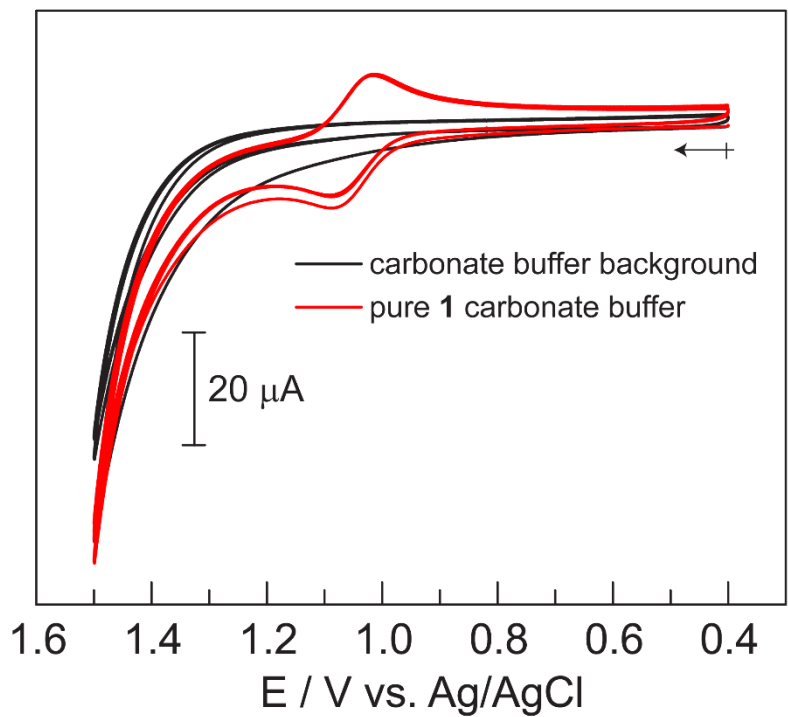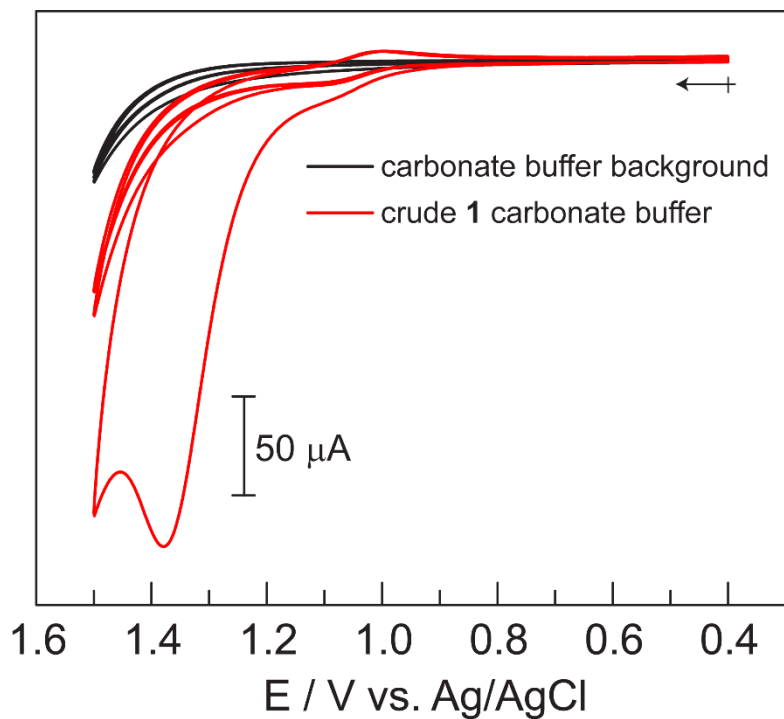
Figure S9. CVs (red line, —) comparing (top) crude **1** (0.852 mg/mL) and (bottom) purified **1** (0.852 mg/mL) in 0.2 M carbonate buffer. The background CVs (black line, —) are provided for comparison.
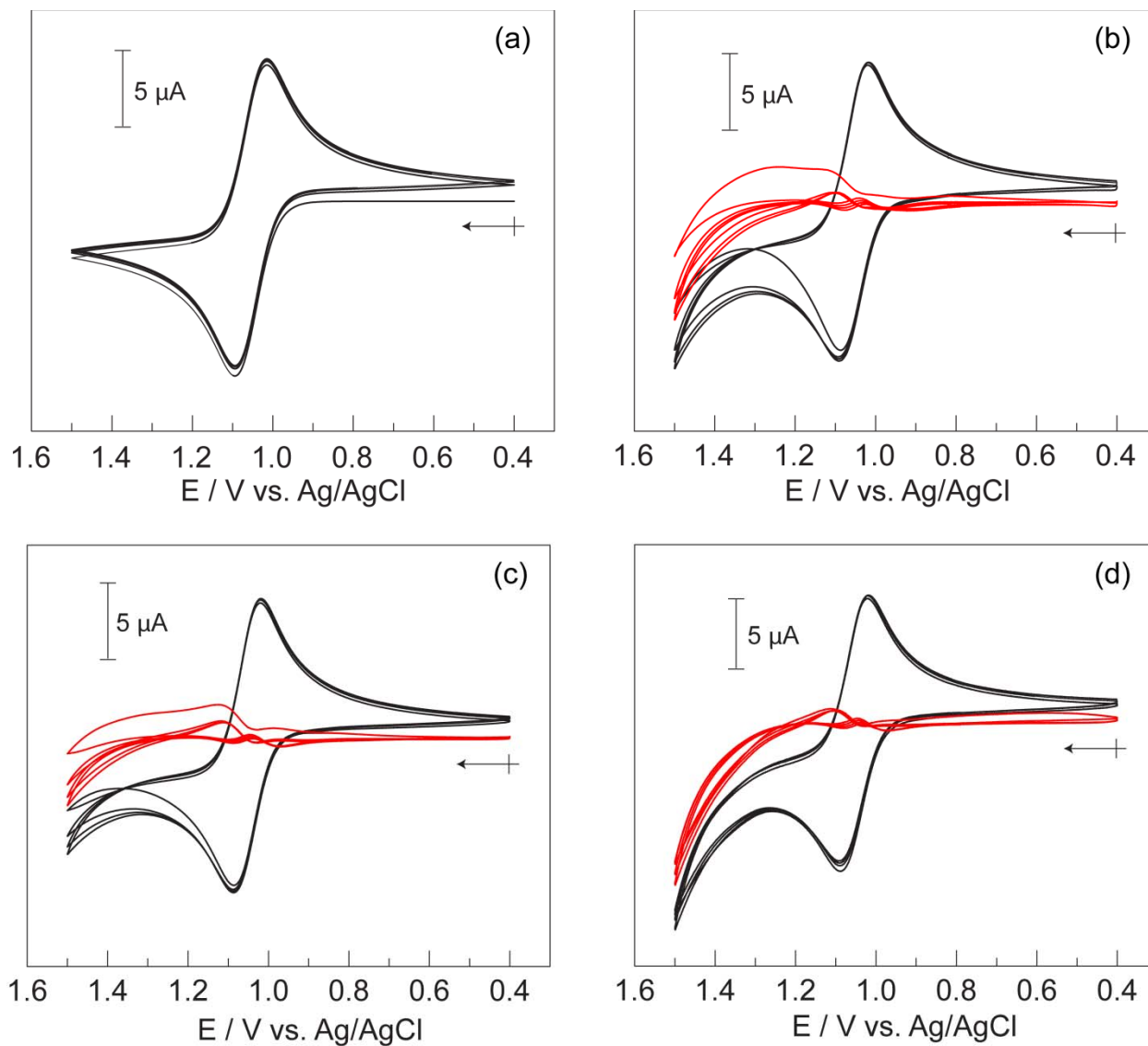
Figure S10. (a) Simulated CV for the Co(IV)Co(III)$_3$/Co(III)$_4$ reversible couple with a E$_{1/2}$ = 1.054 V, a standard rate constant, k_s = 0.008 cm/s, and a diffusion coefficient, D = 4 × 10^{-6} cm^2/s. (b–d) Background subtracted CV traces (black line, ▬) and simulation subtracted CV traces (red line, ▬) of three sample of purified **1** using three independently prepared GC electrodes. The arrows and crosses indicate the initial point and direction of scans. Four full scans are shown for each trace. The oscillating waves in the red traces of b–d (at ~ 1.1 V) are the residual current from imperfect removal of the simulated CV trace.
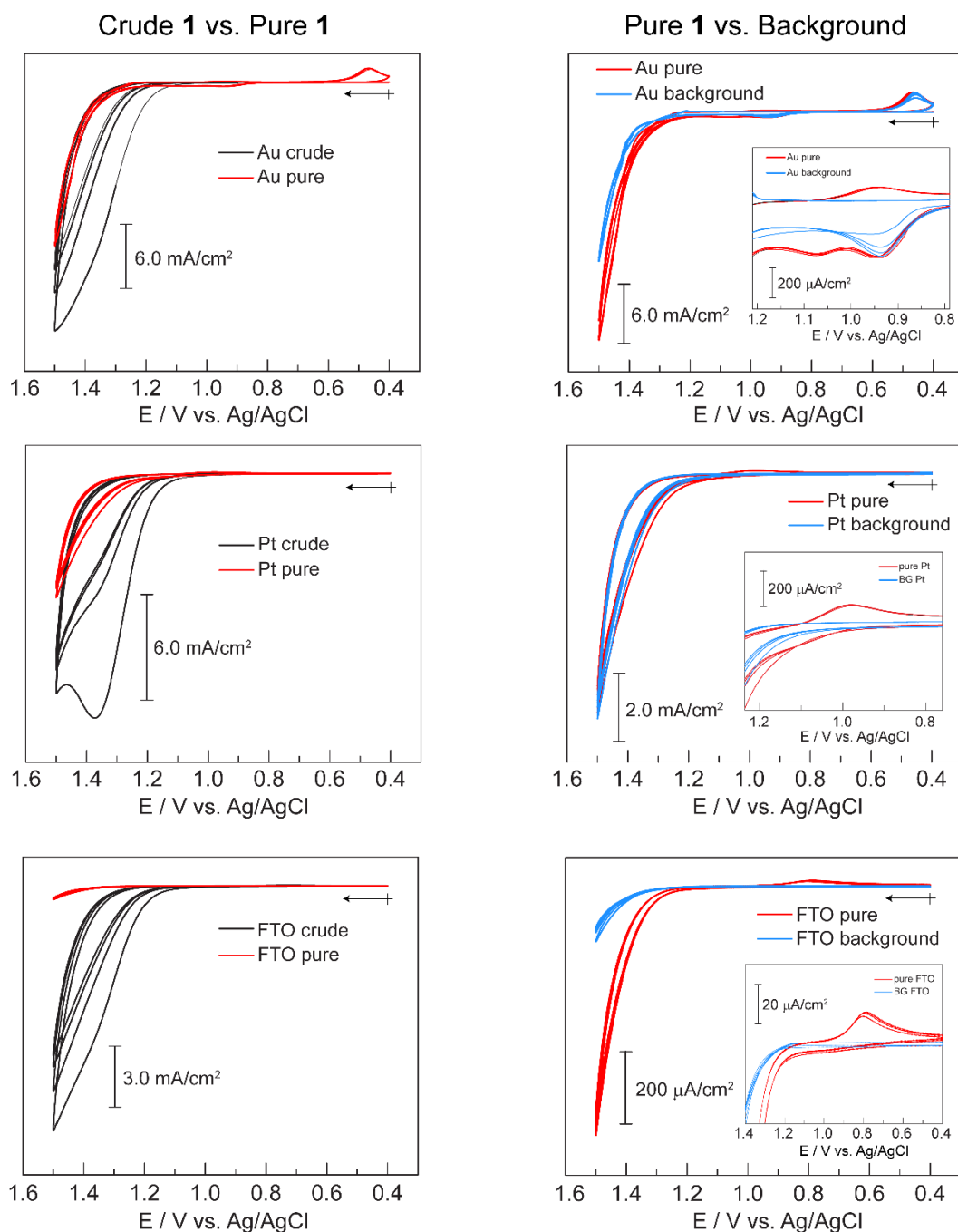
Figure S11. (left) A comparison of CV traces for crude (black line, ▬) and purified **1** (red line, ▬) and right, a comparison of CV traces for purified **1** and background (blue line, ▬) with four full scans shown for each trace using three different electrode materials; Au (top), Pt (middle), and FTO (bottom). The insets on the right side are a magnification of the potential region for the reversible $Co(IV)Co(III)_3/Co(III)_4$ couple. For all experiments the amount of sample is 0.852 mg/mL and the electrolyte is 0.2 M KPi at pH = 7. The arrows and crosses indicate the initial point and direction of scans.
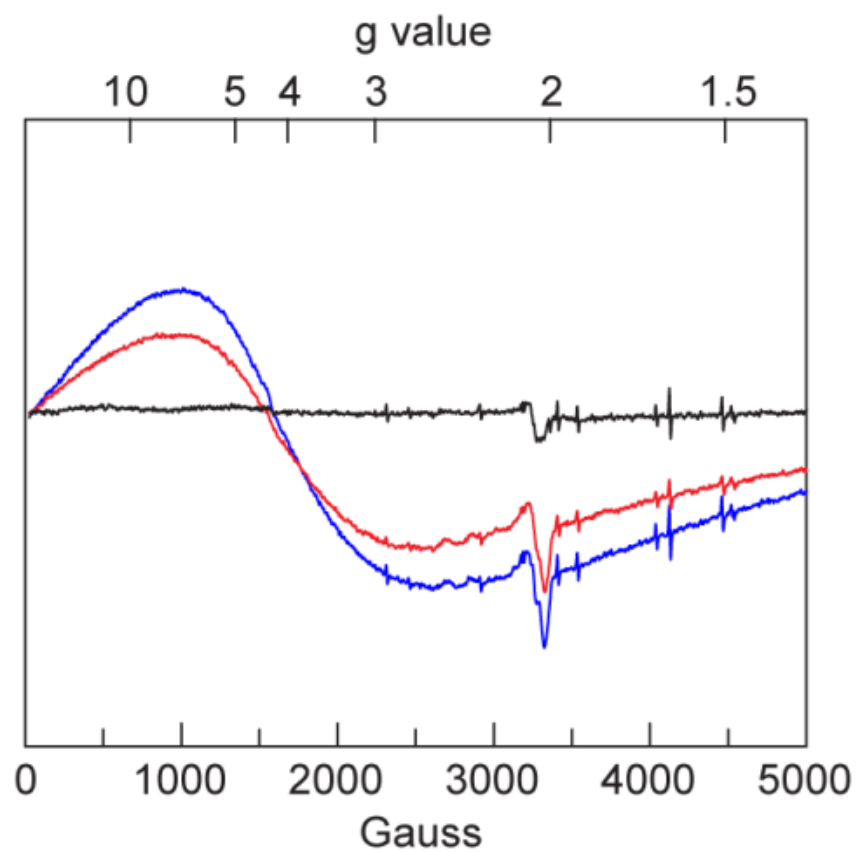
Figure S12. EPR spectra of solid samples of (blue line, —) crude **1** (Batch A), (red line, —) crude **1** (Batch C), and (black line, —) purified **1** with 2 mW microwave power and at 70 K.
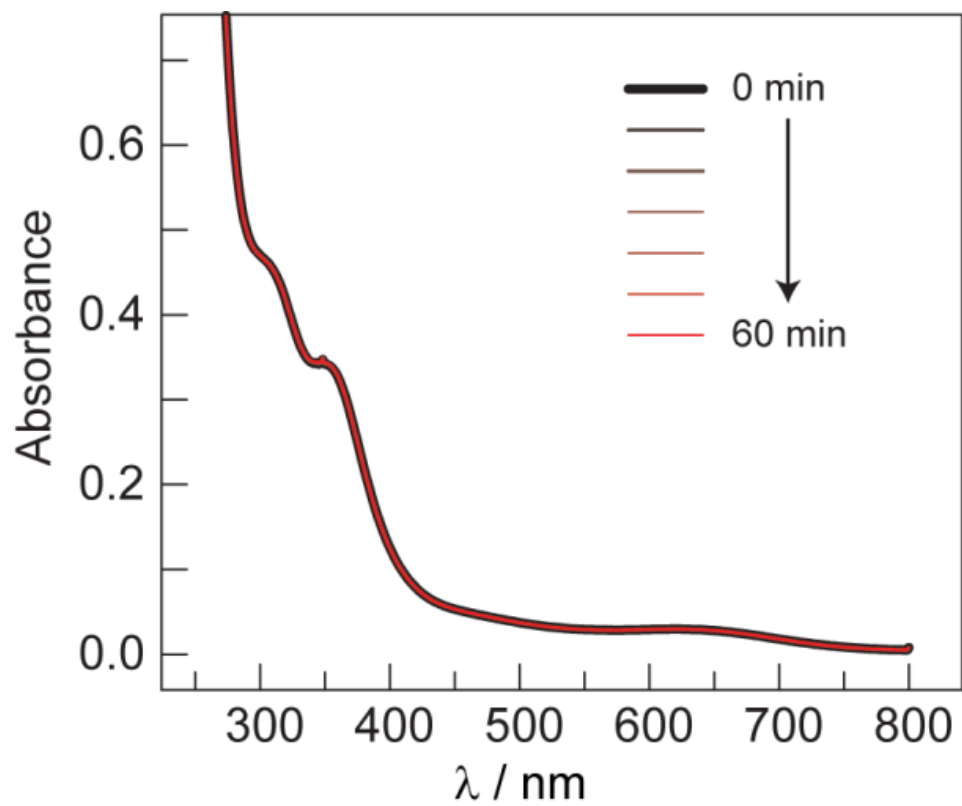
Figure S13. UV-Vis absorption spectra of 0.05 mM of purified **1** in the presence of 10 mM EDTA in 0.2 M KP$_i$ (pH = 7). The perfect overlay of spectra indicates that **1** is stable to EDTA over the course of the 60 min experiment.
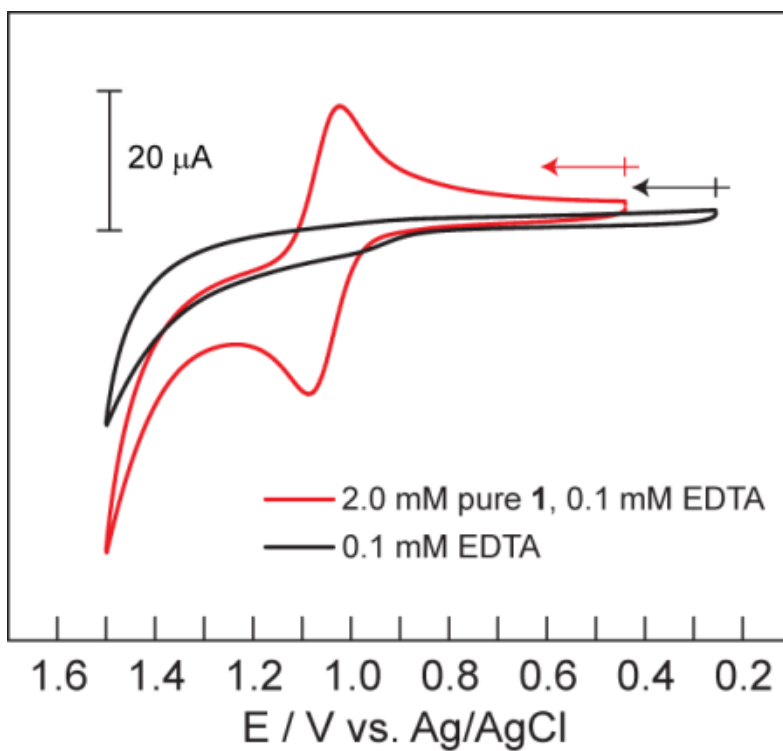
Figure S14. CVs of (red line, ▬) 2 mM of purified **1** in the presence of 0.1 mM EDTA and (black line, ▬) only 0.1 mM EDTA in 0.2 M KP$_i$ (pH = 7). Arrows and crosses indicate the initial point and direction of scans. The downturn in current at high potentials is present in both CVs, indicating that the current is due to EDTA.
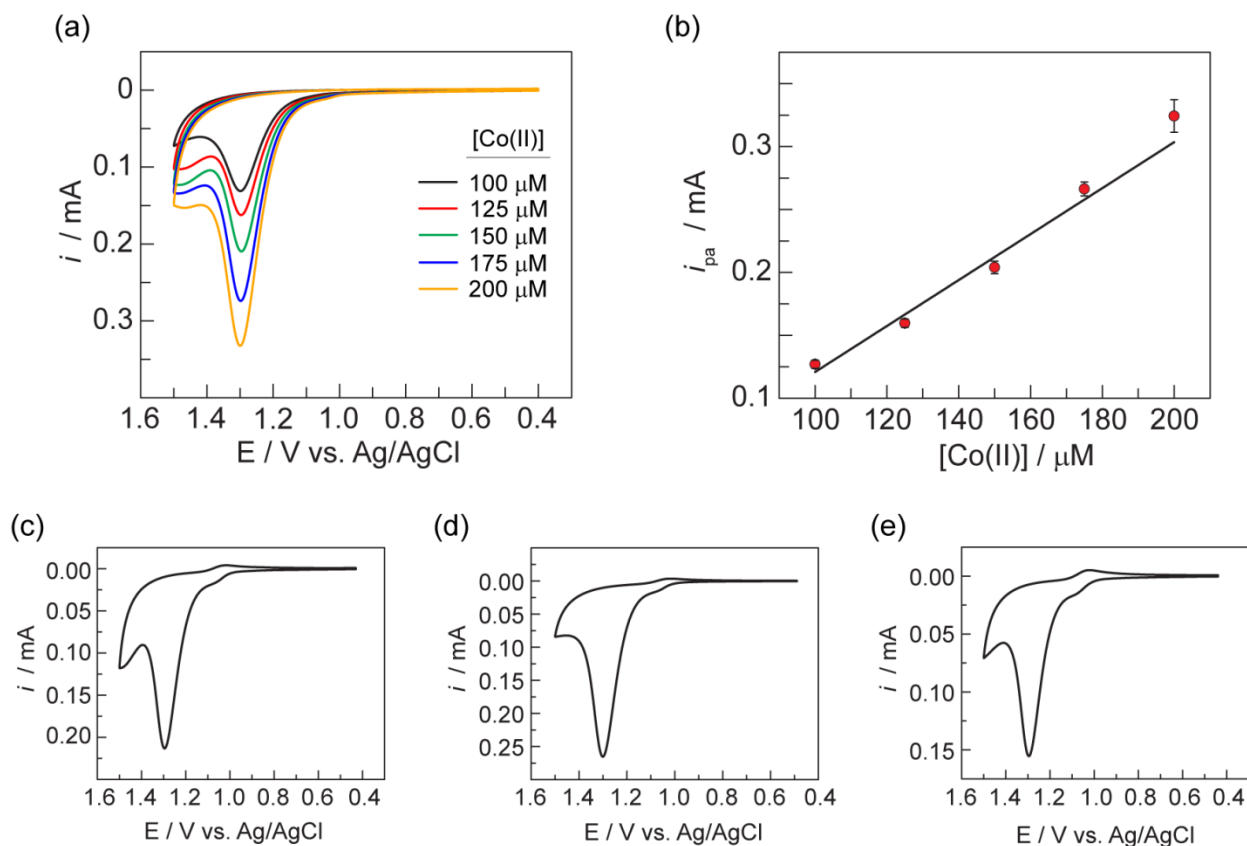
Figure S15. (a) CVs of 1:1 mixtures of Co(OAc)$_2$:pyridine in 0.2 M KP$_i$ (pH = 7) at the indicated concentrations of [Co(II)]; two more measurements were performed (not shown). (b) Linear least squares fit of the average of the three titration measurements with error bars to indicate one standard deviation. The measured current at peak of the catalytic wave is linearly dependent on the concentration of added Co(II). The equation of the linear calibration curve is i_{pa} = (0.018 ± 0.002) × [Co(II)] + (−0.6 ± 0.2). (c–e) CVs of 0.852 mg/mL of crude **1** in 0.2 M KP$_i$ (pH = 7). Using the calibration curve, the measured current at the peak of the catalytic wave was [Co(II)] = 0.153 ± 0.019 mM, 0.178 ± 0.020 mM and 0.120 ± 0.016 mM for (c–e), respectively.
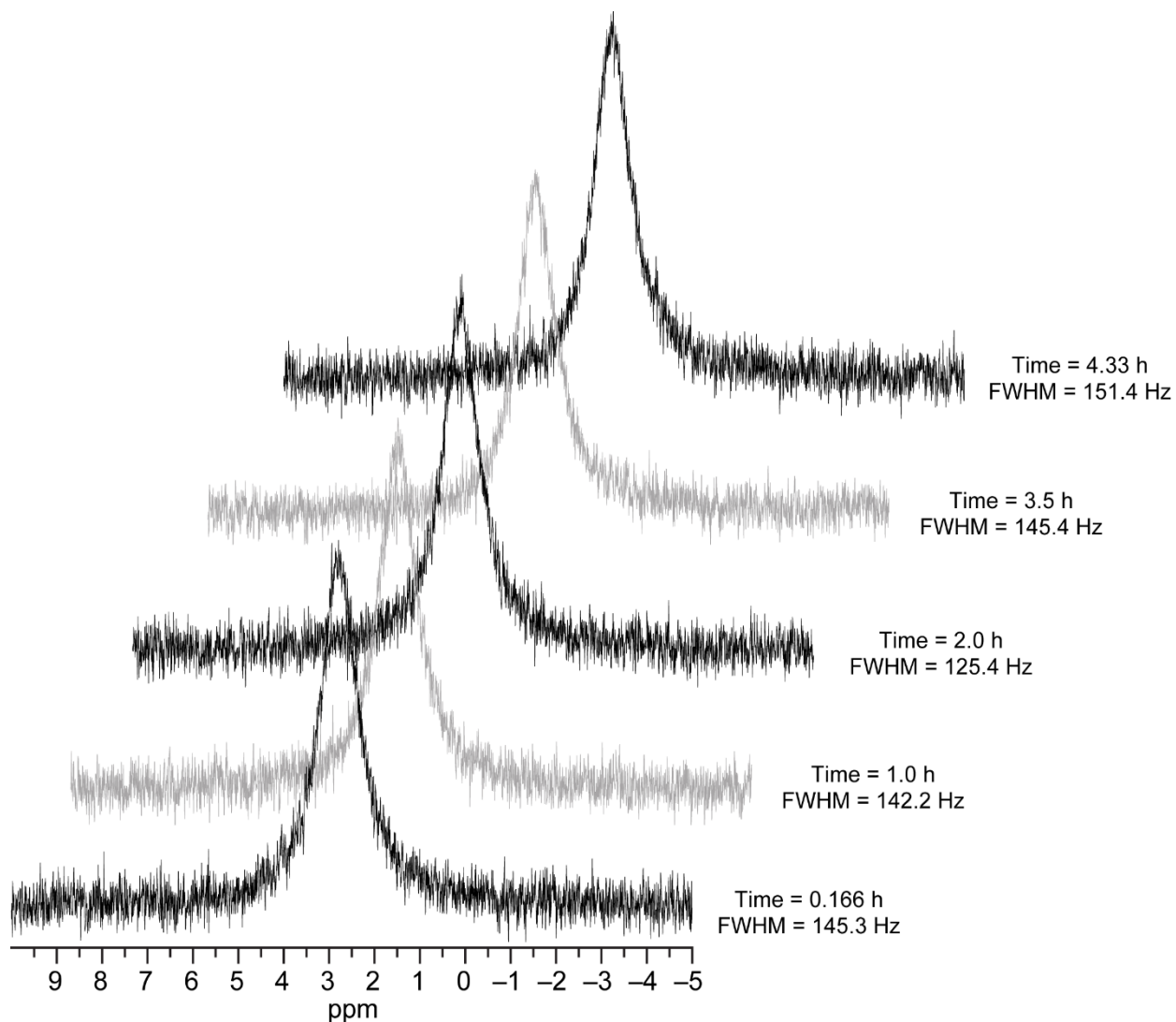
Figure S16. ^{31}P NMR spectra and full width at half max (FWHM) measurements of the phosphate signal of a solution of 0.15 mM Co(OAc)$_2$:pyridine mixture in a 1:1 ratio in a 0.2 M KP$_i$ (pH = 7) solution. The spectra were recorded at the indicated times from when the solution was made.
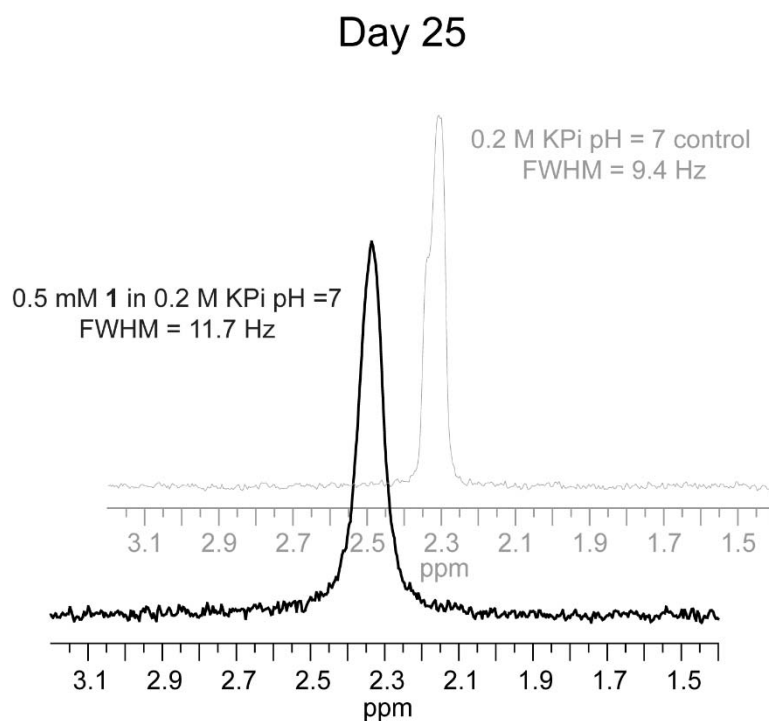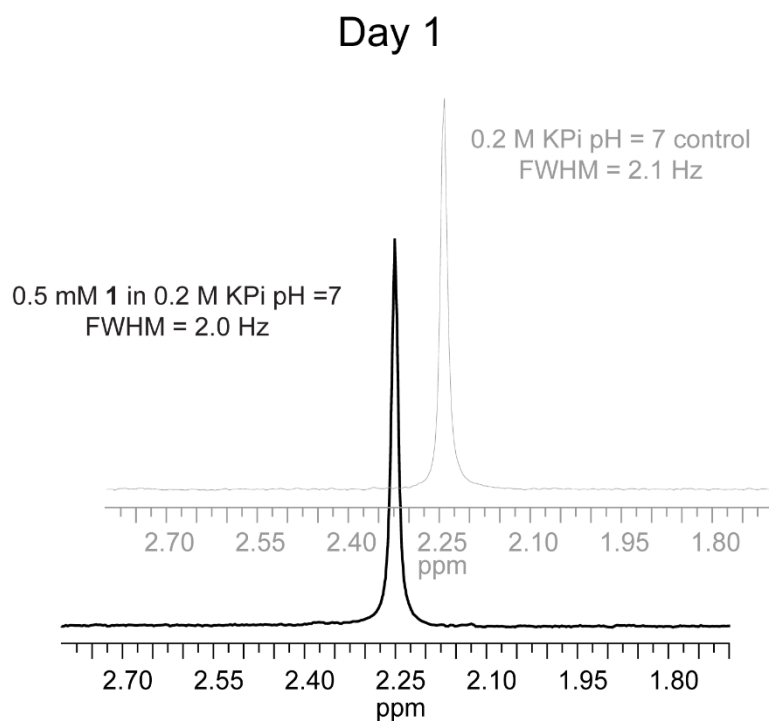
Day 1

0.2 M KPi pH = 7 control
FWHM = 2.1 Hz

0.5 mM **1** in 0.2 M KPi pH =7
FWHM = 2.0 Hz

2.70   2.55   2.40   2.25   2.10   1.95   1.80
ppm

2.70   2.55   2.40   2.25   2.10   1.95   1.80
ppm

Day 25

0.2 M KPi pH = 7 control
FWHM = 9.4 Hz

0.5 mM **1** in 0.2 M KPi pH =7
FWHM = 11.7 Hz

3.1   2.9   2.7   2.5   2.3   2.1   1.9   1.7   1.5
ppm

3.1   2.9   2.7   2.5   2.3   2.1   1.9   1.7   1.5
ppm

Figure S17. ^{31}P NMR spectrum of 0.5 mM purified **1** in 0.2 M KPi buffer at pH = 7 in H_2O day 1 (top) and after storing the compound for 25 days (bottom) under ambient condition in the solid state. The spectra in grey are controls with samples made from buffer solution only. These controls are needed to account for day-to-day variability in the probe response. Note the x-axis has been greatly magnified as compared to Figure 7c–e.
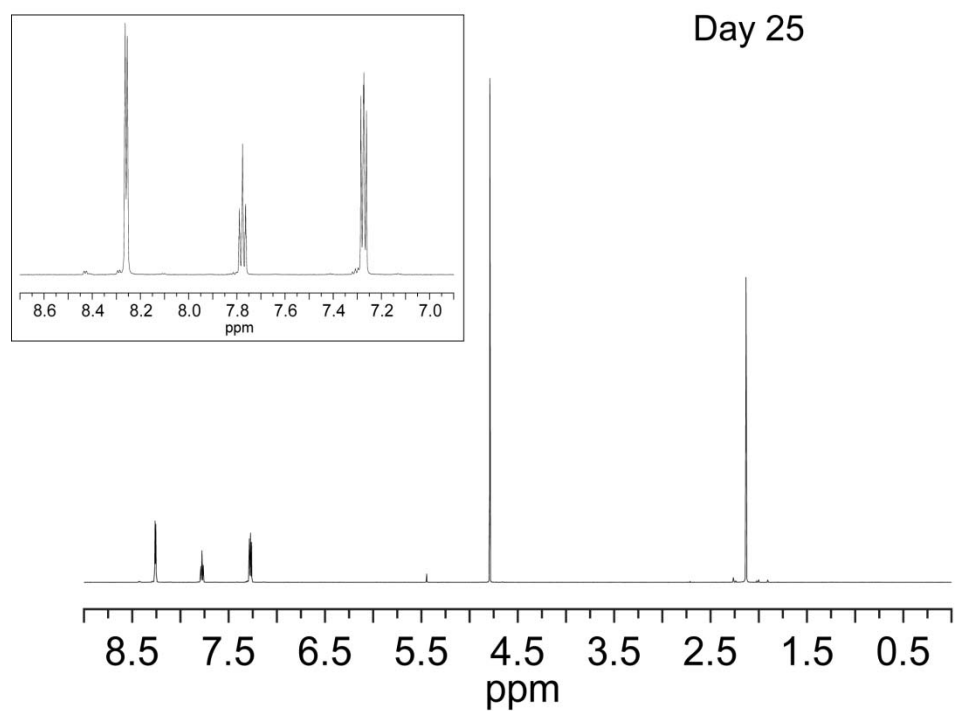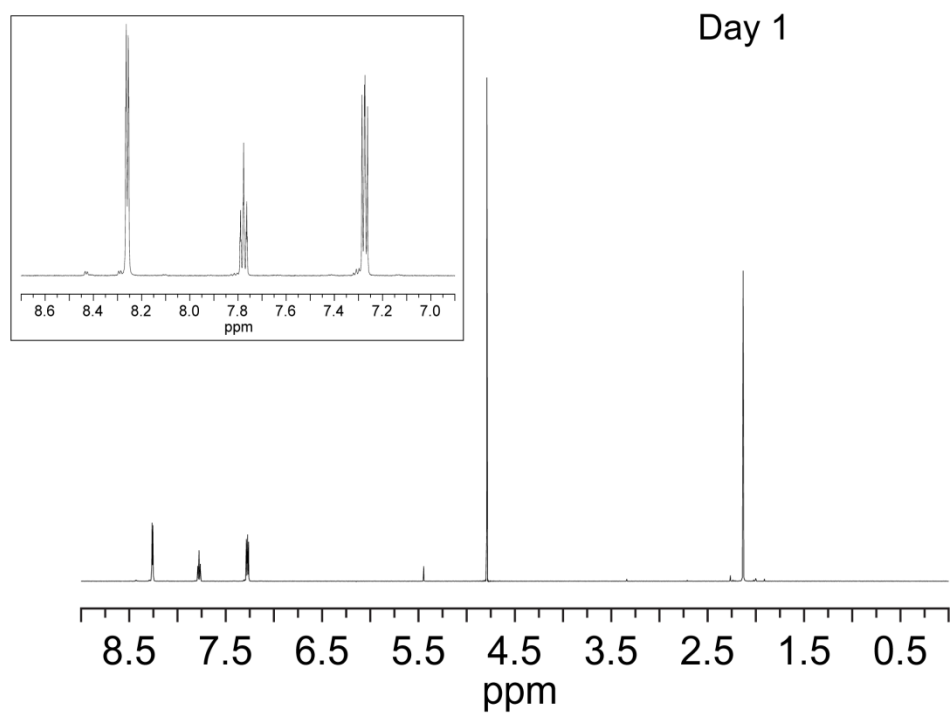
Figure S18. ^{1}H NMR spectrum of 10 mM purified **1** in D_2O (top) day 1 and (bottom) after storing the compound for 25 days under ambient condition in the solid state. Insets: Magnification of the aromatic region of the spectra.
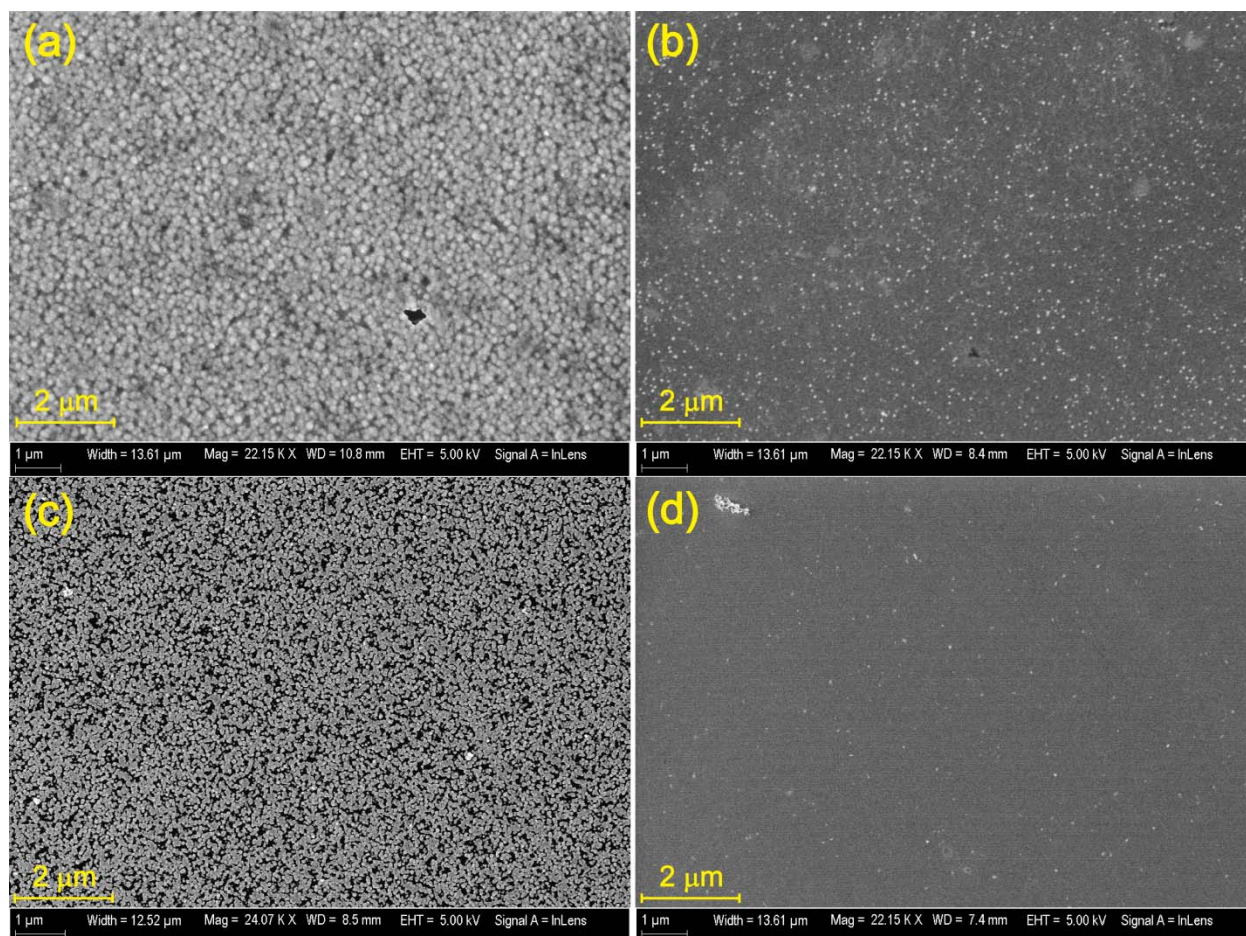
Figure S19. SEM images of GC electrodes after a 300 s bulk electrolysis of (a) crude **1** at 1.2 V, (b) purified **1** at 1.2 V, (c) crude **1** at 1.4 V, and (d) no analyte.
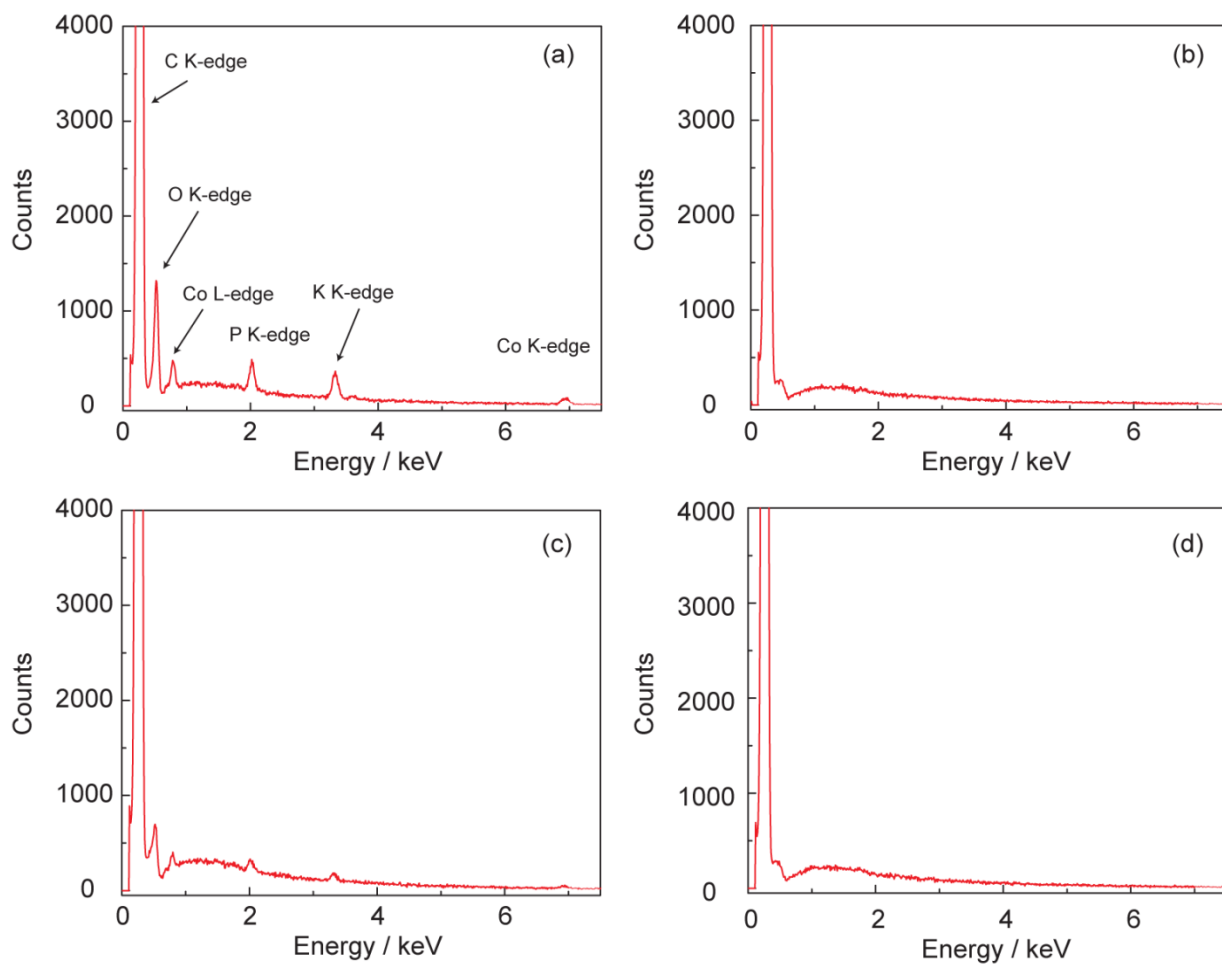
Figure S20. EDS spectra of GC electrodes after a 300 s bulk electrolysis of (a) crude **1** at 1.2 V with labeled edges, (b) purified **1** at 1.2 V, (c) crude **1** at 1.4 V, and (d) no analyte at 1.2 V.
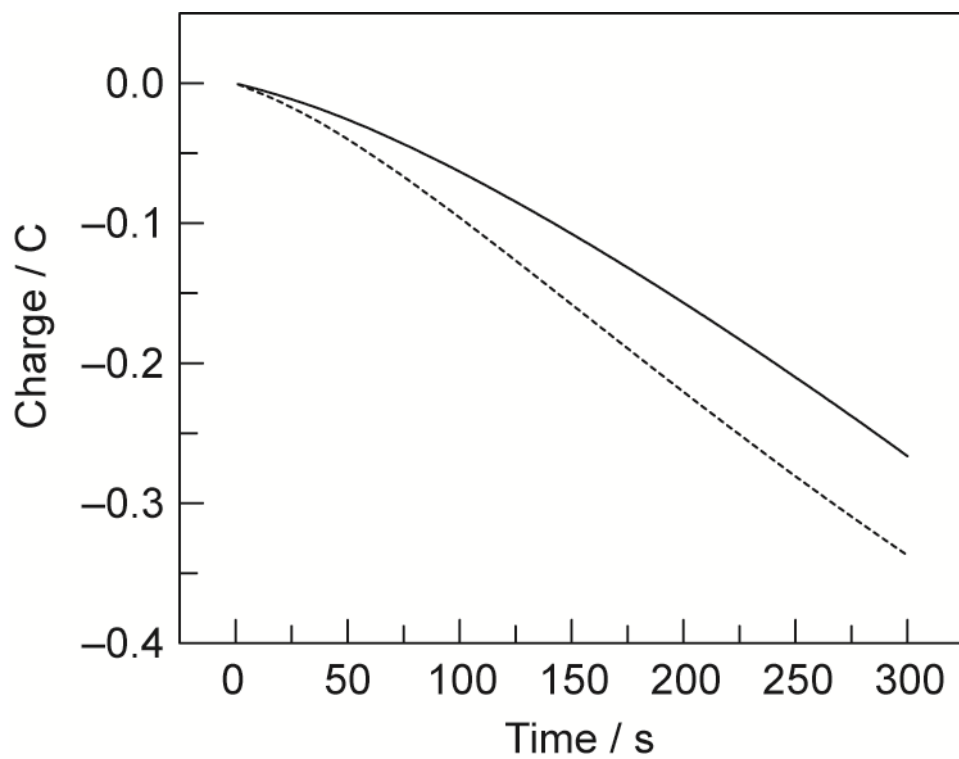
Figure S21. Charge versus time profile for the 300 s bulk electrolysis of (black solid line, ▬) crude **1** at 1.2 V and (black dotted line, •••) of crude **1** at 1.4 V.
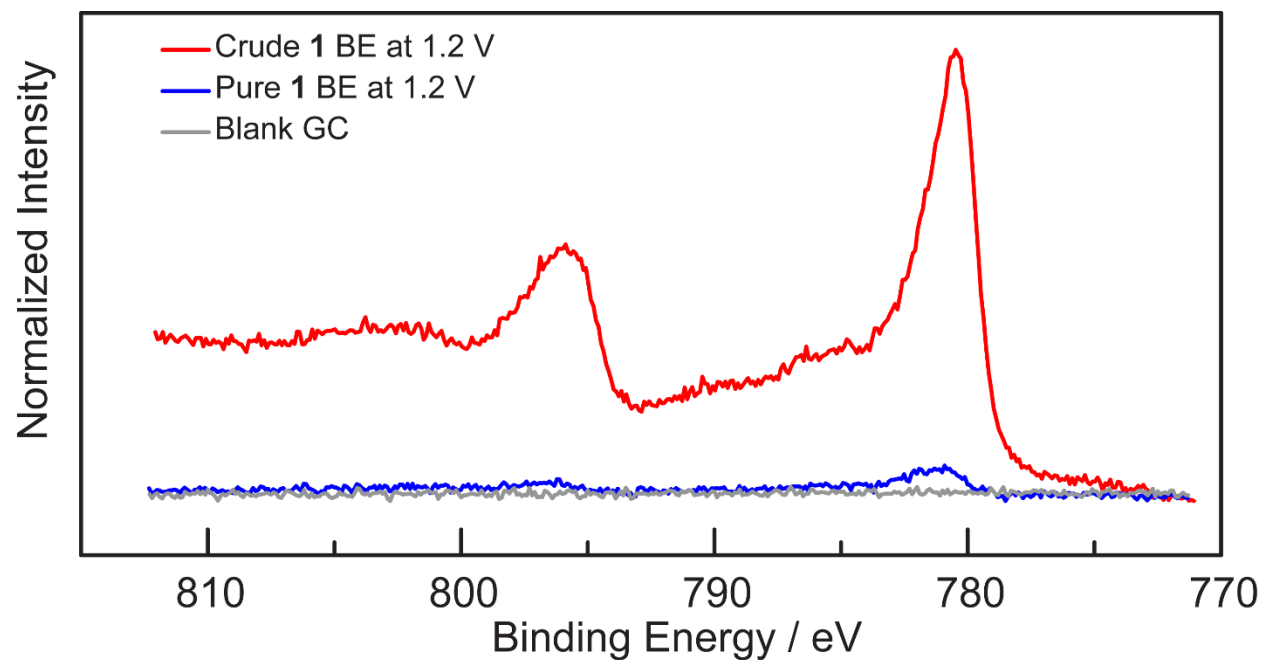
Figure S22. High resolution XPS spectra of the Co $2p_{1/2}$ and $2p_{3/2}$ region of GC electrodes after a 300 s bulk electrolysis of (red line, ▬) crude **1** (Batch A) at 1.2 V, (blue line, ▬) purified **1** at 1.2 V, and (grey line, ▬) no analyte at 1.2 V.
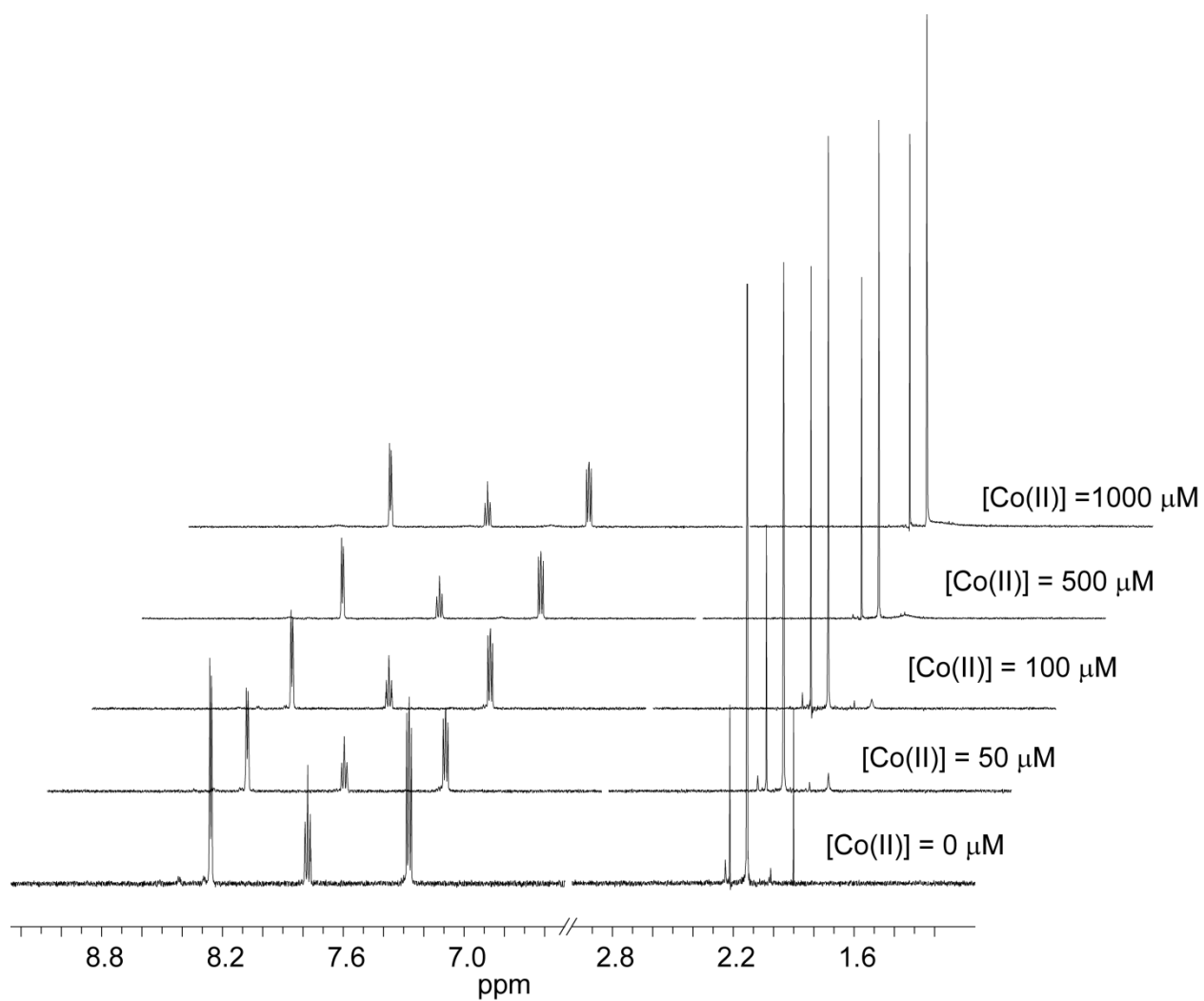
Figure S23. ^1H NMR spectra of 1 mM purified **1** in D_2O with the indicated concentration of Co(II) added in the form of a 1:1 $Co(OAc)_2$:pyridine mixture. Note that there is no significant broadening of any of the proton signals of **1**.
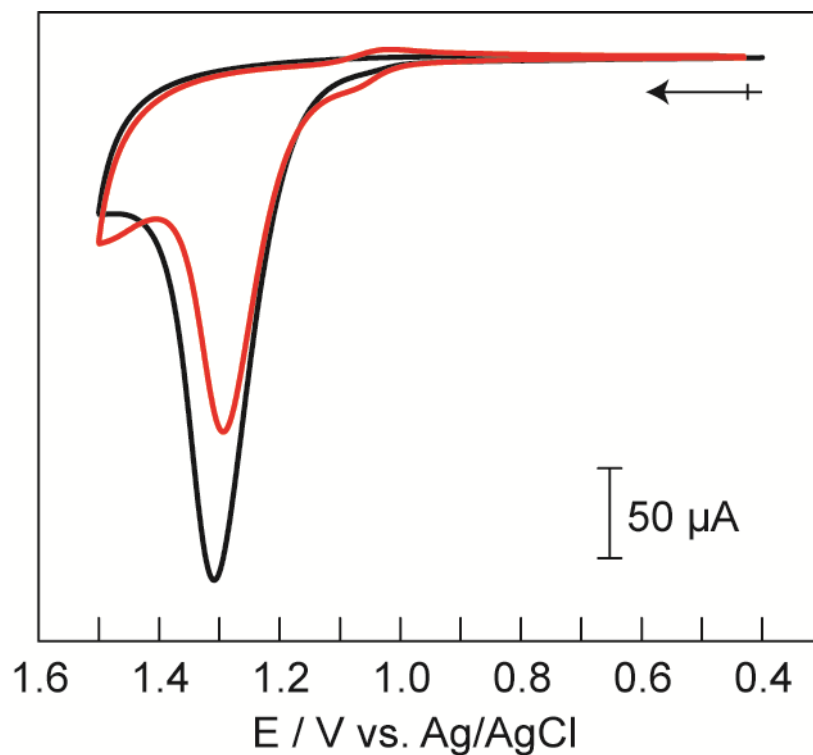
Figure S24. Comparison of CV using a GC electrode of a 0.852 mg/mL sample of crude **1** (—, red line) to a CV obtained from a solution of 150 μM $Co(NO_3)_2$ in 0.2 M KP_i pH = 7 buffer = (—, black line). The profiles of the catalytic currents for the two samples. The pre-feature to the catalytic current of solutions of **1** is the $Co(III)_3Co(IV)/Co(III)_4$ reversible couple of the cubane.[3]
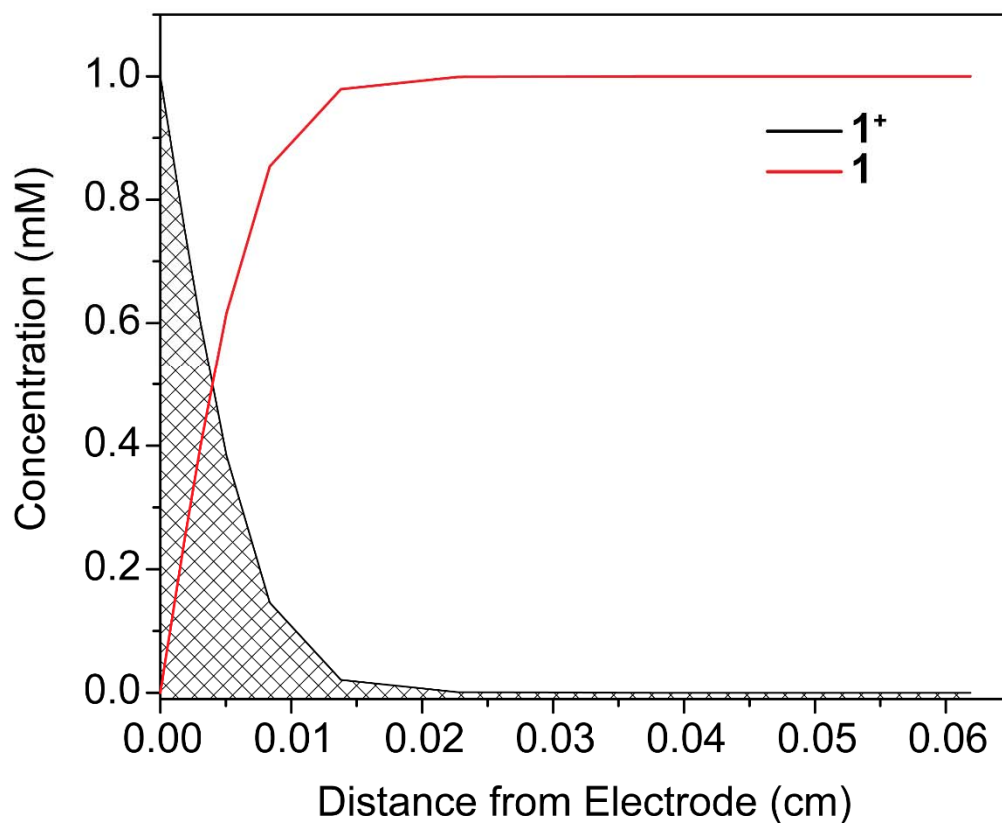
Figure S25. Concentration profile of the simulated CV shown in Figure S10A at 1.5 V vs. Ag/AgCl. The hash marks indicates the integrated area of 4.85 nmol/cm² used to calculate how much cubane experienced the electrode potential during a linear sweep to 1.5 V.